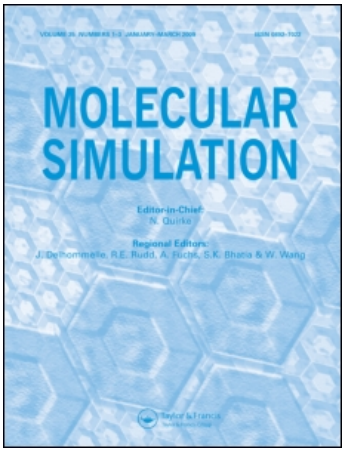

Molecular Simulation
Publication details, including instructions for authors and subscription information:
http://www.informaworld.com/smpp/title~content=t713644482

Fragment replica-exchange method for efficient protein conformation sampling

M. Suzuki[a]; H. Okuda[a]
[a] Research into Artifacts, Center for Engineering (RACE), University of Tokyo, Kashiwa, Chiba, Japan

To cite this Article Suzuki, M. and Okuda, H.(2008) 'Fragment replica-exchange method for efficient protein conformation sampling', Molecular Simulation, 34: 3, 267 — 275
To link to this Article: DOI: 10.1080/08927020701810583
URL: http://dx.doi.org/10.1080/08927020701810583

Molecular Simulation
Vol. 34, No. 3, March 2008, 267–275

Taylor & Francis
Taylor & Francis Group

Fragment replica-exchange method for efficient protein conformation sampling

M. Suzuki* and H. Okuda

Research into Artifacts, Center for Engineering (RACE), University of Tokyo, Kashiwa, Chiba, Japan

(Received 1 March 2007; final version received 13 November 2007)

The native structure of proteins corresponds to the global minimum of the free energy. The replica-exchange method (REM) has been recently used to search for the energy minimum in a wide protein conformation space. For large systems, however, applying REM can be costly because the number of replicas required for conformational sampling increases. We have developed a variant of REM called fragment REM, which is based on the existence of correlations between the local amino acid sequence and the local structure. Equilibrium distributions for two peptides were computed by conventional molecular dynamics, REM and the proposed REM simulations. We found that the modified REM successfully reduces the number of replicas needed for the simulation.

Keywords: fragment replica-exchange method; conformation sampling; protein structure prediction; replica-exchange method

1. Introduction

Proteins are biopolymers in which between a few dozen and a several thousand amino acids are linked together in a chain. A protein folds into its unique native conformation under physiological conditions. Its biological functions are closely related to its conformations; hence, the analysis of protein tertiary structure is very important for post-genomic research.

It is widely believed that molecular simulation will be a powerful tool for elucidating the molecular mechanism of protein folding phenomena. Many researchers have recently attempted to predict protein structures using computer simulations (for a recent review see [1]) along with X-ray structure analysis and other experiments. Computational protein structure prediction is based on the following hypotheses, known as Anfinsen's dogma [2]:

(1) Protein tertiary structure is determined solely by the amino acid sequence information.
(2) Native protein structure corresponds to the global minimum of the free energy.

Therefore, assuming that the accurate energy function of the system is given, the native conformation of proteins can be calculated using methods similar to genetic algorithms, the Monte Carlo (MC), or the molecular dynamics (MD).

Predicting protein structure solely from its amino acid sequence remains a difficult challenge. One of the reasons for the difficulty is the need for massive molecular simulations because direct summation algorithms for calculating long-distance interactions such as electrostatic terms requires $O(N^2)$ operations, where N is the number of atoms included in the system. Although the cutoff method has long been in use for computing N-body interactions, abrupt cutoff results in serious problems related to the stability of the structure and dynamics (e.g. [3,4]). While variant cutoff methods with smooth truncation of forces have been developed (e.g. [5,6]), simulations without the truncation are needed. In addition, it is essential to explicitly incorporate water molecules into the simulation as a solvent to obtain a correct stable state, but this leads to a further increase in the computational cost. Thus, fast summation algorithms and efficient parallel implementations are crucial to performing large-scale biomolecular dynamics simulations. For this purpose, we have adopted Anderson's method [7], a variant of the fast multipole method [8], as a fast summation algorithm, and we applied the hierarchical parallel programming model to this algorithm using a symmetric multiprocessor cluster such as the earth simulator. The effectiveness of the hierarchical programming model has been previously demonstrated [9].

Another reason that it has been difficult to predict protein structure solely from its amino acid sequence is the need for an efficient sampling method that enables searching for the energy minimum in a huge conformational space. Because the number of possible conformations for each protein is immense, each protein can exist in many states corresponding to the local energy minima. Because the thermal fluctuations at low

*Corresponding author. Email: msuzuki@race.u-tokyo.ac.jp

ISSN 0892-7022 print/ISSN 1029-0435 online

DOI: 10.1080/08927020701810583
http://www.informaworld.com

temperatures are small, conventional MD simulations in the canonical ensemble would be trapped in one of these states. One way to tackle this multiple-minima problem is to perform a simulation based on the non-Boltzmann probability weight factors so that a random walk in the energy space can be realised. Compared to the conventional methods, the random walk allows the simulation to pass any energy barrier and to sample a much wider phase space. Of these methods, the replica-exchange method (REM) [10] is well suited to parallel computing.

REM was originally developed by Hukushima and Nemoto [10] for spin glass simulation in the framework of MC simulations. Sugita and Okamoto [11] applied REM to protein systems and combined REM with MD (see [12] for a detailed description of the algorithm). REM considers a number of non-interacting copies (or replicas) of the original system in the canonical ensemble at different temperatures. A REM simulation is realised by alternately performing the following two steps: (i) each replica is simulated simultaneously and independently; and (ii) the pairs of replicas at neighbouring temperatures are exchanged based on Metropolis-type criteria. In this way, simulations can escape from metastable states, but, as explained in Section 3, applying REM to large systems becomes costly because the number of replicas required for conformational sampling increases.

To overcome this difficulty, we have developed a variant of REM called fragment REM (FREM), which is based on the idea that there are correlations between the local amino acid sequence and the local structure. Using peptide simulations, we compare the sampling performance between constant temperature MD, conventional REM and FREM.

2. Replica-exchange methods [10–12]

Let us consider a system of N atoms with their coordinate vectors and momentum vectors, denoted by $\mathbf{q} \equiv \{\mathbf{q}_1, \ldots, \mathbf{q}_N\}$ and $\mathbf{p} \equiv \{\mathbf{p}_1, \ldots, \mathbf{p}_N\}$, respectively. The Hamiltonian $H(\mathbf{q}, \mathbf{p})$ of the system is the sum of the kinetic energy $K(\mathbf{p})$ and the potential energy $E(\mathbf{q})$:

$$H(\mathbf{q}, \mathbf{p}) = K(\mathbf{p}) + E(\mathbf{q}). \tag{1}$$

In the canonical ensemble, at inverse temperature β, each state $\mathbf{x} \equiv \{\mathbf{q}, \mathbf{p}\}$ with the Hamiltonian $H(\mathbf{q}, \mathbf{p})$ is weighted by the Boltzmann factor:

$$W_B(\mathbf{x}) = \exp\{-\beta H(\mathbf{q}, \mathbf{p})\}. \tag{2}$$

The system for REM consists of M non-interacting copies of the original system in the canonical ensemble at M different temperatures T_m $(m = 1, \ldots, M)$. Let $\mathbf{X} = (\mathbf{x}^{[1]}_{m(1)}, \ldots, \mathbf{x}^{[M]}_{m(M)})$ represent a state in this generalised ensemble. The state $\mathbf{X}$ is specified by the M sets of coordinates $\mathbf{q}^{[i]}$ and momenta $\mathbf{p}^{[i]}$ of N atoms in replica i $(i = 1, \ldots, M)$ at temperature T_m:

$$\mathbf{x}^{[i]}_m \equiv (\mathbf{q}^{[i]}, \mathbf{p}^{[i]})_m. \tag{3}$$

Because the replicas are non-interacting, the weighting factor for the state $\mathbf{X}$ in this generalised ensemble is given by the product of Boltzmann factors for each replica:

$$W_{\mathrm{REM}}(\mathbf{X}) = \exp\left\{-\sum_{i=1}^{M} \beta_{m(i)} H(\mathbf{q}^{[i]}, \mathbf{p}^{[i]})\right\}. \tag{4}$$

We now consider exchanging a pair of replicas in the generalised ensemble. Suppose replicas i and j which are at temperatures T_m and T_n, respectively, are exchanged:

$$\begin{aligned}\mathbf{X} &= \left(\ldots, \mathbf{x}^{[i]}_m, \ldots, \mathbf{x}^{[j]}_n, \ldots\right) \rightarrow \mathbf{X}' \\ &= \left(\ldots, \mathbf{x}^{[j]'}_m, \ldots, \mathbf{x}^{[i]'}_n, \ldots\right).\end{aligned} \tag{5}$$

For this exchange process to converge towards the equilibrium distribution, it is sufficient to impose the detailed balance condition on the transition probability $w(\mathbf{X} \rightarrow \mathbf{X}')$ as:

$$W_{\mathrm{REM}}(\mathbf{X}) w(\mathbf{X} \rightarrow \mathbf{X}') = W_{\mathrm{REM}}(\mathbf{X}') w(\mathbf{X}' \rightarrow \mathbf{X}). \tag{6}$$

From Equations (1), (4) and (6), we obtain

$$\frac{w(\mathbf{X} \rightarrow \mathbf{X}')}{w(\mathbf{X}' \rightarrow \mathbf{X})} = \exp(-\Delta), \tag{7}$$

where

$$\Delta \equiv [\beta_n - \beta_m](E(\mathbf{q}^{[i]}) - E(\mathbf{q}^{[j]})). \tag{8}$$

This can be satisfied, for instance, by the usual Metropolis criterion:

$$\begin{aligned} w(\mathbf{X} \rightarrow \mathbf{X}') &\equiv w\left(\mathbf{x}^{[i]}_m \middle| \mathbf{x}^{[j]}_n\right) \\ &= \begin{cases} 1 & \text{for} \quad \Delta \le 0 \\ \exp(-\Delta) & \text{for} \quad \Delta > 0 \end{cases} \end{aligned} \tag{9}$$

A REM simulation is realised by alternately performing the following two steps:

Step 1. Computation of each replica is performed simultaneously and independently for a certain number of MD steps.

Step 2. Pairs of replicas at neighbouring temperatures are exchanged with the transition probability given by Equation (9).

3. Issues for large-scale REM

Exchanges between adjacent replicas should be accepted frequently for efficient conformational sampling. The relationship between the number of replicas and the degrees of freedom in the simulated system has been previously estimated [13]. Considering the potential energy fluctuations of two replicas sampling at each target temperature T_n and T_{n-1} (Figure 1), their instantaneous energy fluctuations δE_n and δE_{n-1} scale as $\sqrt{f}T_n$ and $\sqrt{f}T_{n-1}$, respectively. The average energy gap ΔE between the two neighbouring replicas is proportional to $f\Delta T$. Here, f is the number of degrees of freedom and $\Delta T = T_n - T_{n-1}$. To obtain a reasonable acceptance ratio, the replica energy gap, ΔE, needs to be similar to the energy fluctuations δE_n and δE_{n-1}. Thus, $\Delta E/\delta E$ should be near unity. Because $\Delta E/\delta E$ is proportional to $\Delta T\sqrt{f}/T$ and, hence, $\Delta T \approx 1/\sqrt{f}$, the acceptable temperature gap between the neighbouring replicas becomes narrower as the size of the system increases, and the number of replicas needed increase in proportion to $f^{1/2}$. This implies that for larger systems, more and more replicas are needed and that REM becomes impractical for very large systems such as proteins.

4. FREM

As previously mentioned, a complete amino acid sequence has a one-to-one correspondence with its unique native structure. In addition, the existence of a local correlation between the sequence and structure has been implied by recent studies on knowledge-based protein structure prediction [14].

Motivated by our desire to focus the enhanced sampling on a fraction of the residue fragments of a protein, we proposed a replica-exchange process based on the potential energy of the 'target fragment', *F*. In this study, we defined the residue fragments as depicted in Figure 2. Instead of preparing replicas with different temperatures, in our proposed method, FREM, we

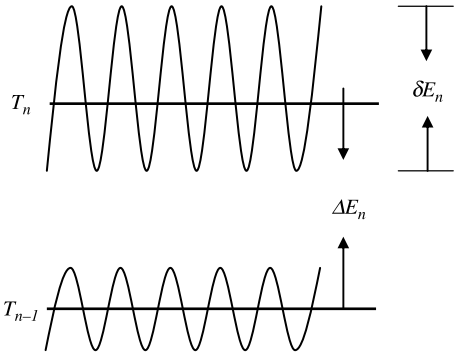

Figure 1. Schematic diagram illustrating the energy fluctuations of simulations at two temperatures for neighbouring replicas.

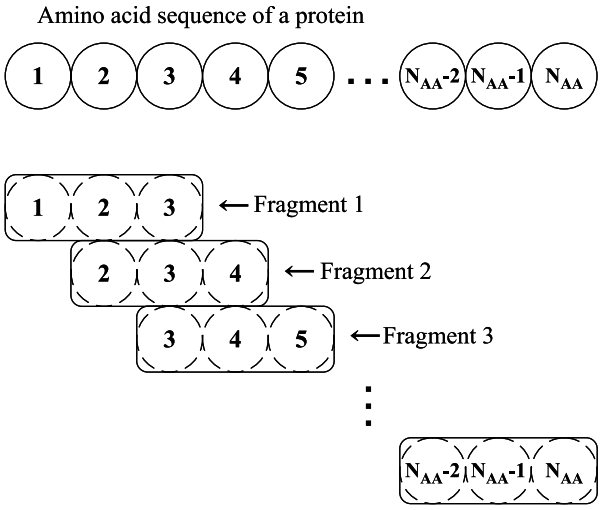

Figure 2. Definition of three-residue length fragments. Each circle represents an amino acid.

introduced replicas with different Hamiltonians. In FREM, the *m*th replica is defined by the Hamiltonian $E_{m(i)}(\mathbf{q}^i)$:

$$E_{m(i)}(\mathbf{q}^i) \equiv S_{m(i)} \sum_{k \in \text{fragment } F} E^k_{AA}(\mathbf{q}^i) + \sum_{k \notin \text{fragment } F} E^k_{AA}(\mathbf{q}^i), \tag{10}$$

where $E^k_{AA}(\mathbf{q}^i)$ is the potential energy of the *k*th amino acid ($k = 1, \ldots, N_{AA}$) in replica *i*, and $S_{m(i)}$ is a scaling factor. This is followed by a procedure similar to that based on the original replica-exchange criterion, resulting in the following transition probability for replica-exchange:

$$w_{\text{FREM}}(\mathbf{x}^i|\mathbf{x}^j) = \begin{cases} 1 & \text{for} \quad \Delta \le 0 \\ \exp(-\Delta_{\text{FREM}}) & \text{for} \quad \Delta > 0 \end{cases}, \tag{11}$$

where

$$\Delta_{\text{FREM}} \equiv \beta(S_{n(j)} - S_{m(i)}) \times \left\{ \sum_{k \in \text{fragment } F} E^k_{AA}(\mathbf{q}^i) - \sum_{k \in \text{fragment } F} E^k_{AA}(\mathbf{q}^j) \right\}. \tag{12}$$

Note that when the target fragment size equals the total number of amino acids, and so the whole Hamiltonian is scaled (that is, $E_m(\mathbf{q}) = S_m E(\mathbf{q})$), it precisely corresponds to the conventional REM with the inverse temperature $\beta_m = \beta S_m$; both give the same Boltzmann factor $\exp\{-\beta S_m E(\mathbf{q})\}$. In FREM, instead of flattening the energy landscape by scaling the whole Hamiltonian, only part of the Hamiltonian specific to the degree of freedoms in the target fragment is weakened by scaling. By doing this, we can change the 'effective temperature' of the partial system. The number of

replicas needed in FREM thus depends solely on the number of degrees of freedom in the target fragment rather than on the size of the whole system, and so the shortage of the conventional REM we mentioned in the previous chapter is overcome.

During the FREM simulation, as shown in Figure 3, only the randomly chosen target fragment is simulated over a range of 'effective temperatures' (in other words, over a range of $S_m\beta$) with periodic exchanges performed according to Equations (11) and (12), while the remainder of the system is maintained at a same temperature for all replicas. After several hundred exchange attempts, the next target fragment is chosen randomly.

Sugita *et al.* [15] proposed a multidimensional extension of REM in which the Hamiltonian of the system depends on a parameter, with different parameter values for different replicas. Fukunishi *et al.* [16] developed an alternative REM called Hamiltonian REM, which is a specific case of multidimensional REM. Although we employ a common approach, this is the first time that the fragment-based expression for the Hamiltonian (Equations (11) and (12)) has been used in this way.

Non-local interaction in the amino acid sequence is the dominant factor for the formation of β-sheet structures, whereas local hydrogen bonding is crucial for α-helices. Thus, it is anticipated that the fragmentation will not work well for a β-sheet structure.

The multiple fragment-size replica-exchange method (MFREM) is a two-dimensional extension of FREM for β-sheet-rich proteins. We treat the 'fragment size' N_ζ ($\zeta = 1, \ldots, N^L_{\mathrm{rep}}$) as second parameter characterising the replicas and write the Hamiltonian for the ith replica as

$$E_{m,\zeta}(\mathbf{q}^i) \equiv S_m \sum_{k \in \text{fragment } F}^{N_\zeta} E^k_{AA}(\mathbf{q}^i) + \sum_{k \notin \text{fragment } F}^{N_{AA}-N_\zeta} E^k_{AA}(\mathbf{q}^i), \tag{13}$$

where $m = 1, \ldots, N^T_{\mathrm{rep}}$ and the total number of replicas $N_{\mathrm{replica}} = N^T_{\mathrm{rep}} \times N^L_{\mathrm{rep}}$. Although replica i and the scaling factor S_m are in one-to-one correspondence in FREM, replica i and the parameter set (S_m, N_ζ) are in one-to-one correspondence in MFREM (Figure 4).

In MFREM, the following replica-exchange processes are performed alternately:

Step 1. Pairs of replicas corresponding to neighbouring temperatures, (S_m, N_ζ) and (S_{m+1}, N_ζ) are exchanged. This is called 'T-exchange'.

Step 2. Pairs of replicas corresponding to 'neighbouring' fragment size, (S_m, N_ζ) and (S_m, $N_{\zeta+1}$) are exchanged. This is called 'L-exchange'.

In each of these two processes, pairs of replicas are simultaneously exchanged, and the pairing is further alternated between the two possibilities. The acceptance criterion for these replica-exchanges is given by

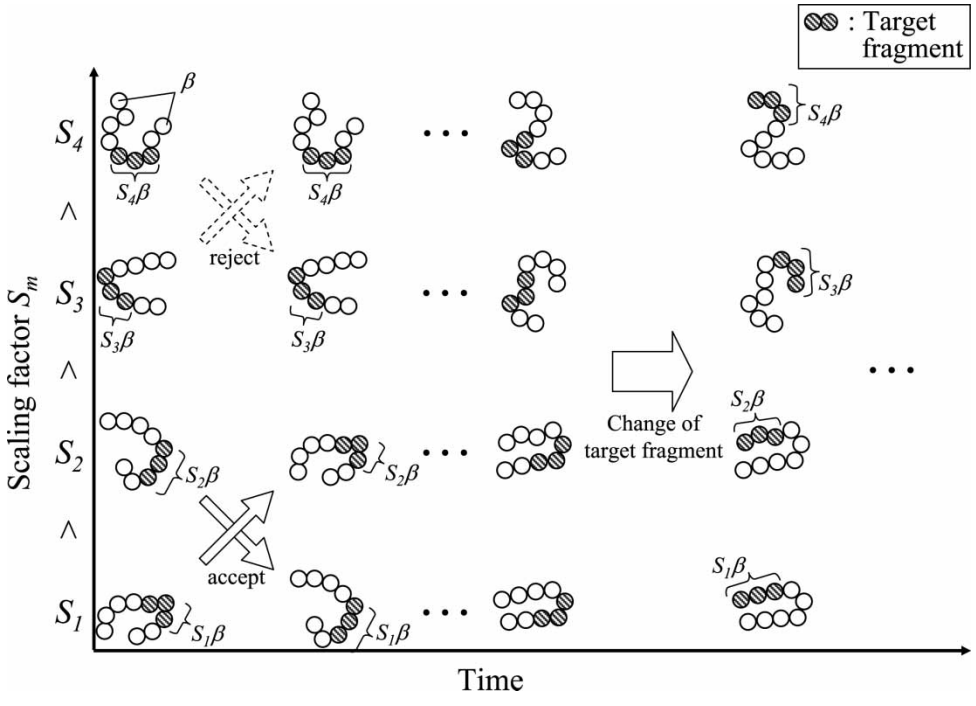

Figure 3. Schematic illustration of the FREM, with four replicas.

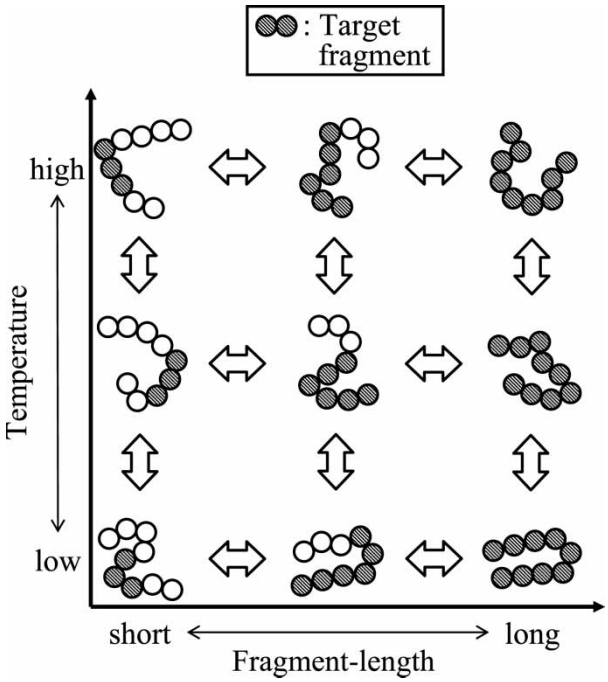

Figure 4. Schematic illustration of the MFREM, with nine replicas.

Equation (9), where Equation (8) now becomes

$$\Delta \equiv \beta\{[E_{m(i),\zeta}(\mathbf{q}^j) + E_{n(j),\zeta}(\mathbf{q}^i)] - [E_{m(i),\zeta}(\mathbf{q}^i) + E_{n(j),\zeta}(\mathbf{q}^j)]\}, \quad (14)$$

for *T*-exchange, and

$$\Delta \equiv \beta\{[E_{m,\zeta(I)}(\mathbf{q}^J) + E_{m,\eta(J)}(\mathbf{q}^I)] - [E_{m,\zeta(I)}(\mathbf{q}^I) + E_{m,\eta(J)}(\mathbf{q}^J)]\}, \quad (15)$$

for *L*-exchange. In MFREM, replica-groups with a small fragment size N_ζ accelerate the local structure refinement. On the other hand, replica-groups with large N_ζ accelerate the global structure refinement.

5. Results and discussion

The sampling efficiency of the proposed methods is discussed using computations for a 16-residue poly-alanine chain and a β-hairpin peptide as examples.

For all calculations, a distance-dependent dielectric, which mimics the presence of a solvent, was used. Electrostatic and van der Waals interactions were calculated without using cutoff by distance, using the direct summation method. The MD time step was set to 0.5 fs. Starting from the fully extended conformation, we performed 250-ps equilibration MD, followed by a 1-ns production MD run.

5.1 α-Helical peptide

The 16-residue poly-alanine peptide predominantly adopts a helical structure below ~300 K. The equilibrium distribution at 200 K was computed using temperature-controlled MD, conventional REM and FREM. The parameters characterising the replicas are summarised in Table 1. For the α-helix peptide simulations, the AMBER ff94 force field [17] was used.

Figure 5 exemplifies how a replica itinerates many target temperatures in FREM with four replicas. Each replica exhibits random walk-like jumps among all target temperatures in FREM, whereas four replicas are not sufficient to obtain efficient exchanges in conventional REM. The histograms of the potential energy for each temperature obtained by the two REMs are shown in Figure 6. For sufficient exchanges between neighbouring replicas, the histograms for adjacent temperatures should demonstrate acceptable overlap. The overlap between the histograms is quite small for conventional REM with four replicas. On the other hand, the histogram pairs with lower temperatures have enough overlap in FREM, although the histograms are unevenly spaced. Table 2 provides the comparison of acceptance ratios of the replica-exchange procedures with four replicas. The acceptance ratios in FREM are significantly larger than those in conventional REM.

Next, we compared the conformational sampling performance by examining the histogram of the total

Table 1. Summary of the replica parameters for the α-helix peptide simulations.

	Conventional REM	FREM
No. of replicas	4, 8, 32	4, 8
Temperatures[a] (K)	(200, 303, 461, 700) for four replicas (200, 239, 286, 342, 409, 489, 585, 700) for eight replicas (200, 208, 217, 226, 235, 245, 255, 265, 276, 288, 299, 312, 325, 338, 352, 366, 382, 397, 414, 431, 448, 467, 486, 506, 527, 549, 571, 595, 620, 645, 672, 700) for 32 replicas	
Replica-exchange interval (fs)	10	
Fragment length (residue)	–	4

[a] For FREM, 'effective temperatures' of target fragment. The remainder of the system is maintained at 200 K.

Table 2. Comparison of acceptance ratios for each REM procedure with four replicas.

	Exchange acceptance ratio	
Temperature pairs (K)	Conventional REM (%)	FREM (%)
200–303	0.004	1.9
303–461	0.006	2.8
461–700	0.008	3.0

potential energy at 200 K (Figure 7). Clearly, regular canonical MD gives different results than the other simulations. This indicates that the regular MD trajectory was trapped in local minima near the initial configuration. As a result, the correct equilibrium distribution was not obtained. The fact that the histograms obtained by conventional REM with four/eight replicas tended to shift to the right with respect to those obtained by conventional REM with 32 replicas indicates that simulations with a few replicas were often trapped in local minima due to low exchange frequencies. This reveals that FREM performs better because the same quality of equilibrium distribution can be achieved with fewer replicas (i.e. four) than the conventional REM (32 replicas).

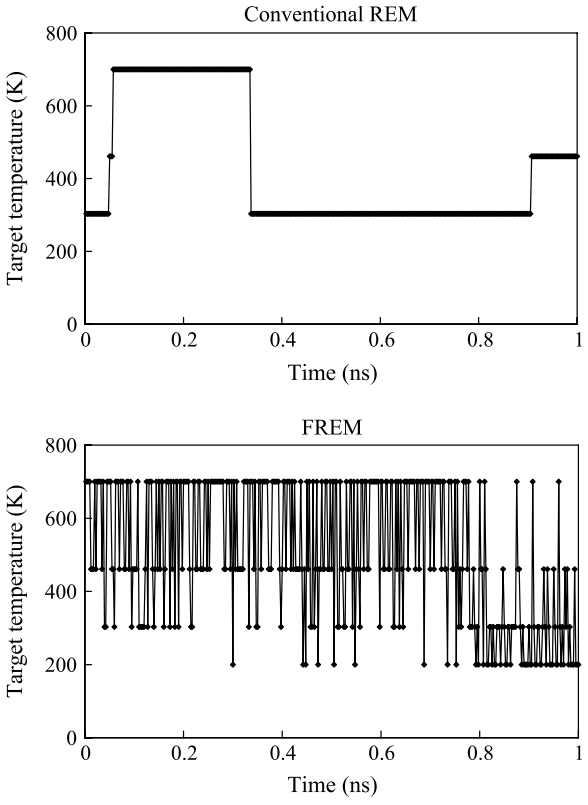

Figure 5. Time series of the target temperatures for one of the replicas obtained by conventional REM (upper) and by FREM (lower) with four replicas.

Figure 8 shows schematic views of the conformational changes in $(ALA)_{16}$ at 200 K obtained by conventional REM and by FREM with four replicas. The structures obtained by FREM are completely helical, whereas those obtained by conventional REM are trapped into misfolded states.

5.2 *β-Hairpin peptide*

We next performed a benchmark test on the β-hairpin peptide Ace-Ile-Thr-Val-Asn-Gly-Lys-Thr-Tyr-Nme. We performed a comparative study similar to that for poly-alanine. For the β-hairpin peptide simulations, the number of replicas was set to eight, and the AMBER ff96 force field [18] was used. The parameters characterising the replicas are summarised in Table 3. In MFREM, eight replicas were simulated at four different temperatures with two different fragment sizes (there are $N^L_{\mathrm{rep}} = 2$ fragment sizes at $N^T_{\mathrm{rep}} = 4$ temperatures, so that the total number of replicas is given by $N_{\mathrm{replica}} = N^T_{\mathrm{rep}} \times N^L_{\mathrm{rep}} = 8$).

Figure 9 shows the time series of target temperatures obtained by three REMs as well as the time series of the target length of the fragment obtained by MFREM for

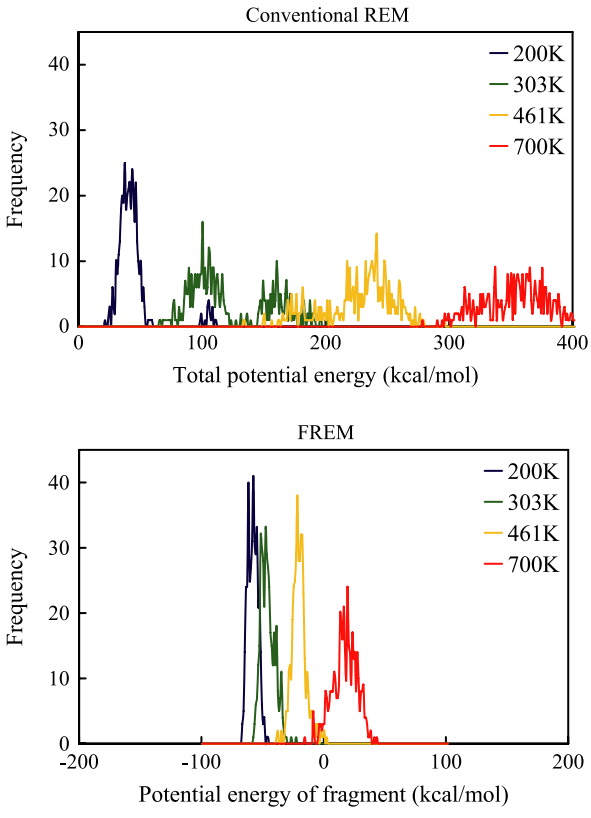

Figure 6. Histogram of the potential energy for each temperature obtained by conventional REM (upper) and FREM (lower) with four replicas.

Table 3. Summary of the replica parameters for the β-hairpin peptide simulations.

	Conventional REM	FREM	MFREM
No. of replicas	8	8	8 ($N^L_{rep} = 2$, $N^T_{rep} = 4$)
Temperatures[a] (K)	(200, 239, 286, 342, 409, 489, 585, 700)		(200, 303, 461, 700)
Replica-exchange interval (fs)	10		
Fragment length (residue)	–	4	4, 10

[a] For FREM and MFREM, 'effective temperatures' of target fragment. The remainder of the system is maintained at 200 K.

one of the replicas. We observed a free random walk in temperature space in both REM variants, whereas MFREM uses only half the number of target temperatures of FREM. Free random walks in 'fragment-size space' were also observed in the MFREM simulation (Figure 9(d)).

Histograms of the total potential energy at 200 K are shown in Figure 10. This analysis reveals that both FREM and MFREM are superior to conventional REM. Moreover, it suggests that MFREM is less often trapped and more efficiently explores the conformational space than FREM. For β-hairpin formation,

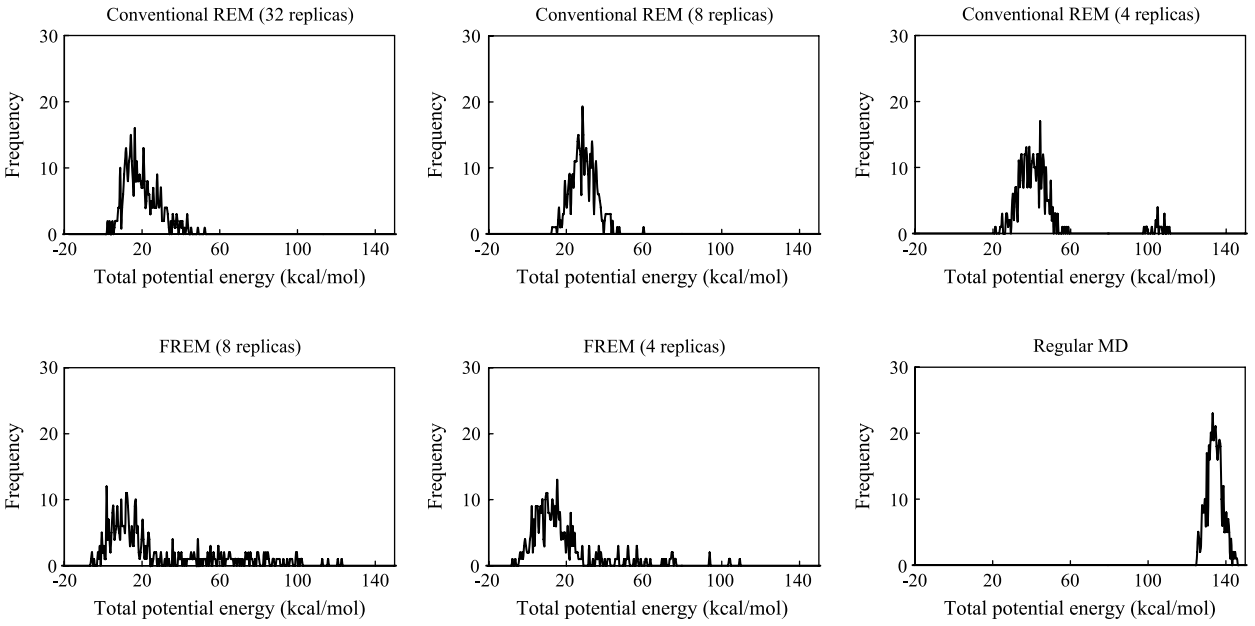

Figure 7. Histogram of the total potential energy at 200 K.

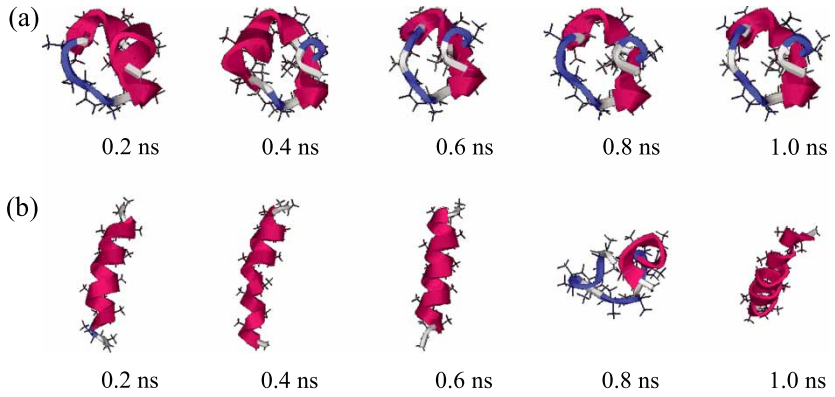

Figure 8. Schematic view of the conformational changes in $(ALA)_{16}$ at 200 K obtained by conventional REM (a) and by FREM (b) with four replicas.

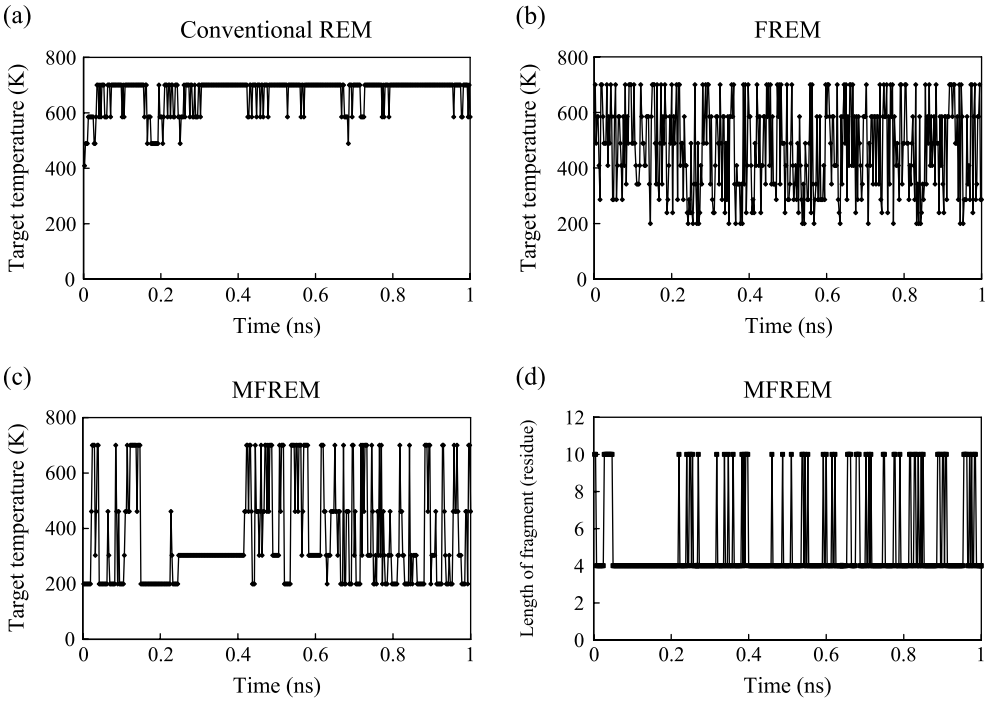

Figure 9. Time series of target temperatures obtained by three REMs (a)–(c) and the time series of the target length of the fragment obtained by the MFREM (d) for one of the replicas.

MFREM introduces global conformation changes due to the variable fragment size, whereas FREM repeats the local structure refinement. This could explain why MFREM seems to be more effective than FREM for β-hairpin peptides. Schematic views of the conformational changes at 200 K for a β-hairpin peptide obtained by conventional REM, FREM, and MFREM are shown in Figure 11. A hairpin conformation is indeed observed in the MFREM simulation (Figures 10 and 11).

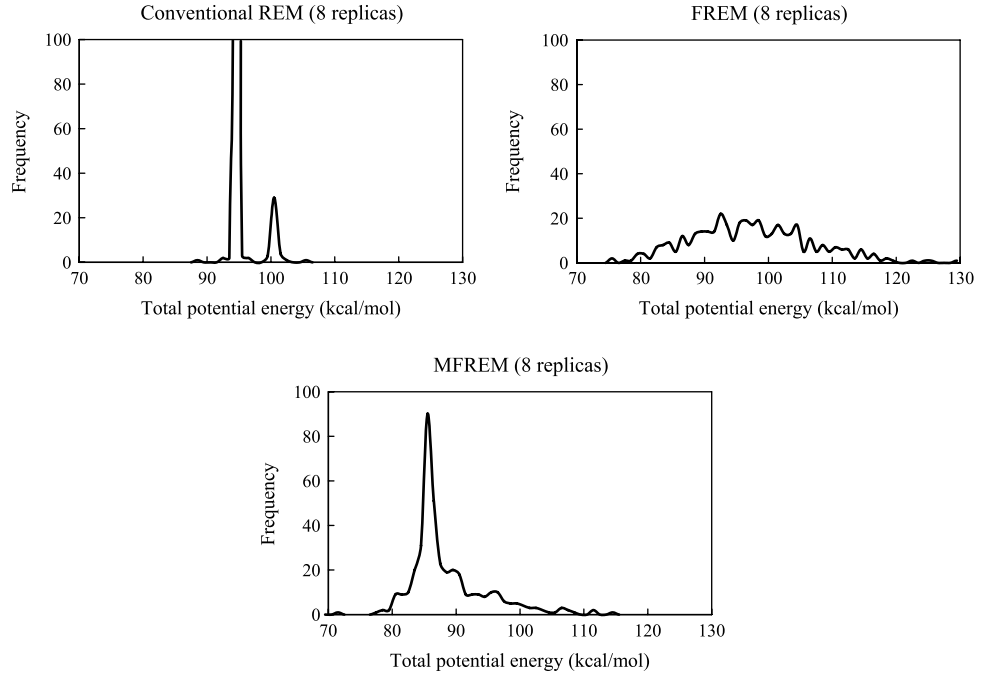

Figure 10. Histogram of the total potential energy at 200 K.

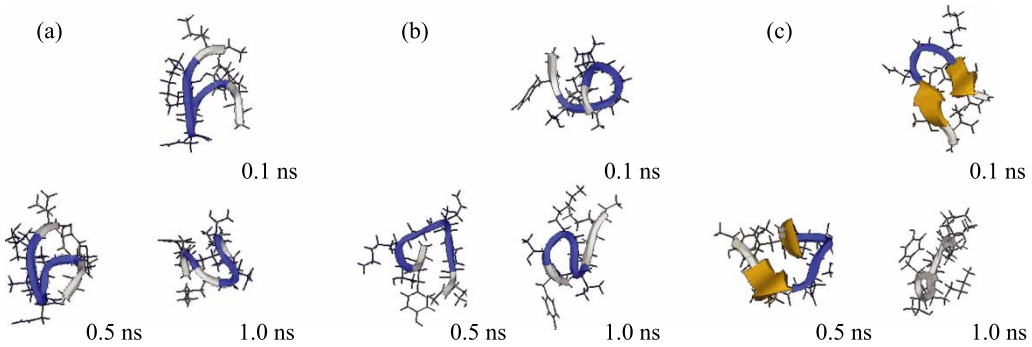

Figure 11. Schematic view of conformational changes in a β-hairpin peptide at 200 K obtained by conventional REM (a), FREM (b) and MFREM (c) with eight replicas.

6. Conclusion

We developed two variants of REM, FREM and MFREM, which are based on the existence of correlations between the local amino acid sequence and the local structure. Equilibrium distributions for two peptides were computed by conventional MD, REM and the proposed REM simulations. We found that both modified REMs successfully reduce the number of replicas needed for the simulation. For small helical peptides, the number of replicas needed in FREM was eight times less than that needed for conventional REM. By introducing global conformation changes, MFREM could sample the conformation space of a β-hairpin peptide more efficiently than FREM.

References

[1] K. Ginalski *et al.*, *Practical lessons from protein structure prediction*, Nucleic Acids Res. 33 (2005), pp. 1874–1891.
[2] C.B. Anfinsen, *Principles that govern the folding of protein chains*, Science 181 (1973), pp. 223–230.
[3] Y. Komeiji *et al.*, *Fast and accurate molecular dynamics simulation of a protein using a special-purpose computer*, J. Comput. Chem. 18 (1997), pp. 1546–1563.
[4] M. Saito, *Molecular dynamics simulations of proteins in solution: artifacts caused by the cutoff approximation*, J. Chem. Phys. 101 (1996), pp. 4055–4061.
[5] D.A.C. Beck *et al.*, *Cutoff size need not strongly influence molecular dynamics results for solvated polypeptides*, Biochemistry 44 (2005), pp. 609–616.
[6] P.J. Steinbach and B. R. Brooks, *New spherical-cutoff methods for long-range forces in macromolecular simulation*, J. Comput. Chem. 15 (1994), pp. 667–683.
[7] C.R. Anderson, *An implementation of the fast multipole method without multipoles*, SIAM J. Sci. Stat. Comput. 13 (1992), pp. 923–947.
[8] L. Greengard and V. Rokhlin, *A fast algorithm for particle simulations*, J. Comput. Phys. 73 (1987), pp. 325–348.
[9] M. Suzuki and H. Okuda, *Acceleration of biomolecular dynamics simulations on the earth simulator*, Int. J. Comput. Methods, in press.
[10] K. Hukushima and K. Nemoto, *Exchange Monte Carlo method and application to spin glass simulations*, J. Phys. Soc. Jpn 65 (1996), pp. 1604–1608.
[11] Y. Sugita and Y. Okamoto, *Replica-exchange molecular dynamics method for protein folding*, Chem. Phys. Lett. 314 (1999), pp. 141–151.
[12] A. Mitsutake *et al.*, *Generalized-ensemble algorithms for molecular simulations of biopolymers*, Biopolymers (Pept. Sci.) 60 (2001), pp. 96–123.
[13] X. Cheng *et al.*, *Modified replica exchange simulation methods for local structure refinement*, J. Phys. Chem. B 109 (2005), pp. 8220–8230.
[14] K.T. Simons *et al.*, *Assembly of protein tertiary structures from fragments with similar local sequences using simulated annealing and Bayesian scoring functions*, J. Mol. Biol. 268 (1997), pp. 209–225.
[15] Y. Sugita *et al.*, *Multidimensional replica-exchange method for free-energy calculations*, J. Chem. Phys. 113 (2000), pp. 6042–6051.
[16] H. Fukunishi *et al.*, *On the Hamiltonian replica exchange method for efficient sampling of biomolecular systems: application to protein structure prediction*, J. Chem. Phys. 116 (2002), pp. 9058–9067.
[17] W.D. Cornell *et al.*, *Second generation force field for the simulation of proteins, nucleic acids and organic molecules*, J. Am. Chem. Soc. 117 (1995), pp. 5179–5197.
[18] D.A. Pearlman *et al.*, *AMBER a package of computer programs for applying molecular mechanics, normal mode analysis, molecular dynamics and free energy calculations to simulate the structural and energetic properties of molecules*, Comput. Phys. Commun. 91 (1995), pp. 1–41.